Separation Science and Technology
Publication details, including instructions for authors and subscription information:
http://www.informaworld.com/smpp/title~content=t713708471

Groundwater Cleanup by *in-situ* Sparging. II. Modeling of Dissolved Volatile Organic Compound Removal

David J. Wilson[a]
[a] DEPARTMENT OF CHEMISTRY, VANDERBILT UNIVERSITY NASHVILLE, TENNESSEE

To cite this Article Wilson, David J.(1992) 'Groundwater Cleanup by *in-situ* Sparging. II. Modeling of Dissolved Volatile Organic Compound Removal', Separation Science and Technology, 27: 13, 1675 — 1690
To link to this Article: DOI: 10.1080/01496399208019440
URL: http://dx.doi.org/10.1080/01496399208019440

SEPARATION SCIENCE AND TECHNOLOGY, 27(13), pp. 1675–1690, 1992

Groundwater Cleanup by *in-situ* Sparging. II. Modeling of Dissolved Volatile Organic Compound Removal

DAVID J. WILSON
DEPARTMENT OF CHEMISTRY
VANDERBILT UNIVERSITY
NASHVILLE, TENNESSEE 37235

Abstract

Simple steady-state and nonsteady-state models are developed for describing the removal of dissolved volatile organic compounds (VOCs) from aquifers by sparging techniques. A method is given for estimating the streamlines and transit times of water in a stagnant or nearly stagnant aquifer in the vicinity of a sparging well, and the resulting flow velocities are used to develop a model for the sparging of a VOC obeying Henry's law.

INTRODUCTION

In a recent paper Herrling and Stamm (*1*) discussed the use of vacuum-vaporizer wells for the *in-situ* removal of volatile organic compounds (VOCs) in the vadose and saturated zones, a technique which is now well-established in Germany. At the same meeting Brown (*2*) described the simple air injection or sparging wells which Ground Water Technology, Inc., has employed in the United States for *in-situ* removal of VOCs from contaminated groundwater. We recently published on an aeration curtain configuration for sparging and the use of vadose zone piezometer measurements to infer the distribution of injected air at the top of the aquifer in the vicinity of a sparging well (*3*). This technology appears to have a good deal of potential utility in the remediation of aquifers contaminated with VOCs, including, apparently, those cases in which nonaqueous phase liquids (NAPLs) are present. It is well known that the presence of dense nonaqueous phase liquids (DNAPLs) in an aquifer represents a very serious challenge to anyone contemplating remediation of the site, and there is some hope that sparging techniques may be effective even in this area.

In connection with sparging, a point of particular interest has been addressed by Weber and his coworkers (*4*); this is the nonequilibrium effects occurring during the solution of "blobs" of NAPL in advecting groundwater. They felt that these were due to 1) rate limited mass transport between the nonaqueous and aqueous phases, 2) the by-passing of advecting aqueous phase around contaminated regions of low permeability, and 3) nonuniform flow due to aquifer heterogeneities.

In the following we address the problem of modeling the removal of dissolved VOCs from an aquifer by sparging. The objective is the development of models sufficiently simple as to permit their ready use on currently available microcomputers. In the second section we present a simple two-compartment steady-state model, which is then extended to deal with the nonsteady-state case in the third section. In the fourth section we examine the question of the water flow patterns in the vicinity of a single sparging well, and in the last section these results are used to develop a somewhat more elaborate model for the sparging of dissolved VOC from an aquifer.

TWO-COMPARTMENT STEADY-STATE MODEL FOR SPARGING

A simple analytical model useful in getting insight into the sparging process is illustrated in Fig. 1. Here contaminated groundwater flows through a large compartment V_1 at a flow rate Q_1. During its stay in V_1 it may exchange at a flow rate Q_2 with water in a second compartment V_2 which is being sparged with air at a flow rate Q_a. Let

c_0 = VOC concentration in the groundwater coming into V_1 (kg/m^3)
c_1 = VOC concentration in V_1 and discharged from V_1 (kg/m^3)
c_2 = VOC concentration in V_2 (kg/m^3)
c_a = VOC concentration in discharged air (kg/m^3)
K_H = VOC Henry's constant (dimensionless)

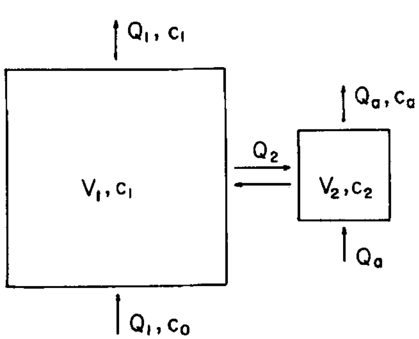

FIG. 1. A simple two-compartment model for the sparging of VOC.

m_1 = mass of contaminant VOC in V_1 (kg)
m_2 = mass of contaminant VOC in V_2 (kg)

Under conditions of steady-state operation we have

$$dm_1/dt = 0 = Q_1(c_0 - c_1) + Q_2(c_2 - c_1) \tag{1}$$

$$dm_2/dt = 0 = Q_2(c_1 - c_2) - Q_aK_Hc_2 \tag{2}$$

where we have utilized Henry's law by setting $c_a = K_Hc_2$. Solution of these equations yields

$$c_1 = \frac{Q_1(Q_2 + Q_aK_H)c_0}{Q_1Q_2 + (Q_1 + Q_2)Q_aK_H} \tag{3}$$

$$c_2 = \frac{Q_1Q_2c_0}{Q_1Q_2 + (Q_1 + Q_2)Q_aK_H} \tag{4}$$

$$c_a = \frac{Q_1Q_2K_Hc_0}{Q_1Q_2 + (Q_1 + Q_2)Q_aK_H} \tag{5}$$

A computer program was written to evaluate these formulas, and some representative simulations were run. Since this type of aeration involves a cross-current configuration, it is essentially a single-stage process, and efficiencies are likely to be relatively low if one uses a realistic value for the dimensionless Henry's constant (around 0.2 for a number of aromatic and chlorinated solvents). Rearrangement of Eq. (3) yields

$$\frac{c_1}{c_0} = \frac{1}{1 + \dfrac{Q_2Q_aK_H}{Q_1(Q_2 + Q_aK_H)}} = R_1 \tag{6}$$

and the percent removal resulting from a single pass through the sparging system is given by

$$(\%\ \text{removal})_1 = (1 - R_1)\cdot 100\% \tag{7}$$

If the values of Q_2 and Q_a necessary to obtain the desired level of VOC removal are excessive, it may be more economical to install an array of

TABLE 1
Two-Compartment Steady-State Sparging Model Using Local Equilibrium and Henry's Law. Parameters and Results

	Run no.						
	1	2	3	4	5	6	7
Q_1, m^3/s	0.001	0.001	0.001	0.001	0.001	0.001	0.001
Q_2, m^3/s	0.002	0.002	0.002	0.005	0.01	0.02	0.05
Q_a, m^3/s	0.01	0.05	0.10	0.10	0.10	0.10	0.10
K_H, dimensionless	0.2	0.2	0.2	0.2	0.2	0.2	0.2
c_0, kg/m^3	1.0	1.0	1.0	1.0	1.0	1.0	1.0
Discharge concn	0.500	0.375	0.355	0.200	0.130	0.0909	0.0654
Effluent gas concn	0.0500	0.0125	0.0065	0.0080	0.0087	0.0091	0.0093

sparging wells so that an element of groundwater passes through the domains of influence of n wells, rather than only one. In this case we have

$$c_n/c_0 = R_1^n \tag{8}$$

so substantially higher removal efficiencies can be obtained without the need to pump enormous quantities of air.

Some representative results obtained with Eq. (6) are shown in Table 1.

TWO-COMPARTMENT NONSTEADY-STATE MODEL FOR SPARGING

The extension of the two-compartment model to nonsteady-state conditions is done as follows. We use the same notation as in the preceding section. The nonsteady-state equations are

$$V_1\frac{dc_1}{dt} = Q_1(c_0 - c_1) + Q_2(c_2 - c_1) \tag{9}$$

$$V_2\frac{dc_2}{dt} = Q_2(c_1 - c_2) - Q_aK_Hc_a \tag{10}$$

We let

$$c_1 = c_1^{ss} + s_1 \tag{11}$$

$$c_2 = c_2^{ss} + s_1 \tag{12}$$

where the superscript *ss* denotes the steady-state solution obtained in the preceding section. The equations for s_1 and s_2 are easily found to be

$$V_1 \frac{ds_1}{dt} = -Q_1 s_1 + Q_2(s_2 - s_1) \tag{13}$$

$$V_2 \frac{ds_2}{dt} = Q_2(s_1 - s_2) - Q_a K_H s_2 \tag{14}$$

This system is readily solved by standard eigenvalue methods; the secular equation for the eigenvalues is

$$\begin{vmatrix} m - \dfrac{Q_1 + Q_2}{V_1} & \dfrac{Q_2}{V_1} \\ \dfrac{Q_2}{V_2} & m - \dfrac{Q_2 + Q_a K_H}{V_2} \end{vmatrix} = 0 \tag{15}$$

The roots of this are

$$m_+ = (b + \sqrt{b^2 - 4c})/2 \tag{16}$$

$$m_- = (b - \sqrt{b^2 - 4c})/2 \tag{17}$$

where

$$b = (Q_1 + Q_2)/V_1 + (Q_2 + Q_a K_H)/V_2 \tag{18}$$

and

$$c = (Q_1 + Q_2)(Q_2 + Q_a K_H)/V_1 V_2 \tag{19}$$

The eigenvectors corresponding to m_+ and m_- can be taken as $\binom{1}{a_+}$ and $\binom{1}{a_-}$, where

$$a_- = \frac{V_1}{Q_2}\left[\frac{Q_1 + Q_2}{V_1} - m_+\right] \tag{20}$$

and

$$a_- = \frac{V_1}{Q_2}\left[\frac{Q_1 + Q_2}{V_1} - m_-\right] \tag{21}$$

The general solution for s_1 and s_2 is then given by

$$\begin{pmatrix} s_1 \\ s_2 \end{pmatrix} = B_+ \begin{pmatrix} 1 \\ a_+ \end{pmatrix} \exp(-m_+t) + B_- \begin{pmatrix} 1 \\ a_- \end{pmatrix} \exp(-m_-t) \tag{22}$$

If we take as our initial conditions that $c_1 = c_2 = c_0$, the contaminant concentration in the unremediated aquifer, B_+ and B_- are given by

$$B_+ = \frac{a_-(c_0 - c_1^{ss}) - (c_0 - c_2^{ss})}{a_- - a_+} \tag{23}$$

$$B_- = \frac{(c_0 - c_2^{ss}) - a_+(c_0 - c_1^{ss})}{a_- - a_+} \tag{24}$$

Finally, the nonsteady-state VOC concentrations in the volumes V_1 and V_2 are given by

$$c_1(t) = c_1^{ss} + B_+ \exp(-m_+t) + B_- \exp(-m_-t) \tag{25}$$

$$c_2(t) = c_2^{ss} + B_+a_+ \exp(-m_+t) + B_-a_- \exp(-m_-t) \tag{26}$$

Some representative results obtained with Eqs. (25) and (26) are given in Table 2.

TABLE 2
Two-Compartment Nonsteady-State Sparging Model, Local Equilibrium, Henry's Law. Parameters and Results

Run #1
Q_1 = .001 m³/s — Incident concn c_0 = 1.00 kg/m³
Q_2 = .005 m³/s — Steady-state discharge concn = .412 kg/m³
V_1 = 20 m³ — Steady-state effluent gas concn = .0588 kg/m³
V_2 = 5 m³ — Henry's constant = .2 (dimensionless)
Q_a = .01 m³/s

Time (s)	c(aqueous discharge) (kg/m³)	c_2 (kg/m³)	c(gas discharge) (kg/m³)
0	1.0000	1.0000	0.2000
100	0.9988	0.9078	0.1816
200	0.9956	0.8276	0.1655
500	0.9765	0.6446	0.1289
1,000	0.9268	0.4682	0.0936
2,000	0.8129	0.3370	0.0674
5,000	0.5787	0.2948	0.0590
10,000	0.4490	0.2941	0.0588
20,000	0.4136	0.2941	0.0588
50,000	0.4118	0.2941	0.0588
100,000	0.4118	0.2941	0.0588

(*continued*)

TABLE 2 (*continued*)

Run #2

Q_1 = .001 m^3/s Incident concn c_0 = 1.00 kg/m^3
Q_2 = .005 m^3/s Steady-state discharge concn = .310 kg/m^3
V_1 = 20 m^3 Steady-state effluent gas concn = .0345 kg/m^3
V_2 = 5 m^3 Henry's constant = .2 (dimensionless)
Q_a = .02 m^3/s

Time (s)	c(aqueous discharge) (kg/m^3)	c_2 (kg/m^3)	c(gas discharge) (kg/m^3)
0	1.0000	1.0000	0.2000
100	0.9983	0.8637	0.1727
200	0.9935	0.7498	0.1500
500	0.9666	0.5089	0.1018
1,000	0.9006	0.3092	0.0618
2,000	0.7607	0.1950	0.0390
5,000	0.4950	0.1725	0.0345
10,000	0.3515	0.1724	0.0345
20,000	0.3124	0.1724	0.0345
50,000	0.3103	0.1724	0.0345
100,000	0.3103	0.1724	0.0345

Run #3

Q_1 = .001 m^3/s Incident concn c_0 = 1.00 kg/m^3
Q_2 = .05 m^3/s Steady-state discharge concn = .412 kg/m^3
V_1 = 20 m^3 Steady-state effluent gas concn = .0588 kg/m^3
V_2 = 5 m^3 Henry's constant = .2 (dimensionless)
Q_a = .1 m^3/s

Time (s)	c(aqueous discharge) (kg/m^3)	c_2 (kg/m^3)	c(gas discharge) (kg/m^3)
0	1.0000	1.0000	0.2000
100	0.8996	0.2818	0.0564
200	0.7390	0.1047	0.0209
500	0.3845	0.0476	0.00952
1,000	0.1546	0.0467	0.00935
2,000	0.0724	0.0467	0.00935
5,000	0.0654	0.0467	0.00935
10,000	0.0654	0.0467	0.00935
20,000	0.0654	0.0467	0.00935
50,000	0.0654	0.0467	0.00935
100,000	0.0654	0.0467	0.00935

GROUNDWATER FLOW PATTERNS IN THE VICINITY OF A SPARGING WELL

The above models have the disadvantage of being rather phenomenological in nature, with parameters which may be conceptually clear but which would in practice be rather difficult to evaluate. In this section we explore the flow patterns which may be expected when an aquifer with little or no natural flow is sparged with a single well.

Consider the situation illustrated in Fig. 2 where we have a sink $-Q$ at the bottom of the aquifer and a source Q at the top of the aquifer, representing the intake of water from the bottom of the aquifer into the bottom of the sparging zone and the discharge of water from the top of the sparging zone back into the top of the aquifer, respectively. We let h be the thickness of the aquifer. This flow field can be approximated by the distribution of sources and sinks shown in Fig. 3 where the hatched region is the domain of interest (the aquifer).

A solution to Laplace's equation corresponding to this distribution of sources and sinks is the following:

$$W = \sum_{n=-\infty}^{\infty} A\left[\frac{2Q}{\sqrt{r^2 + [z - (2n + 1)h]^2}} - \frac{2Q}{\sqrt{r^2 + [z - 2nh]^2}}\right] \tag{27}$$

The constant A is determined by the requirement that

$$2Q = \int_0^{2\pi} \int_0^{\pi} A\frac{2Q}{\rho^2}\rho^2 \sin\theta d\theta d\phi \tag{28}$$

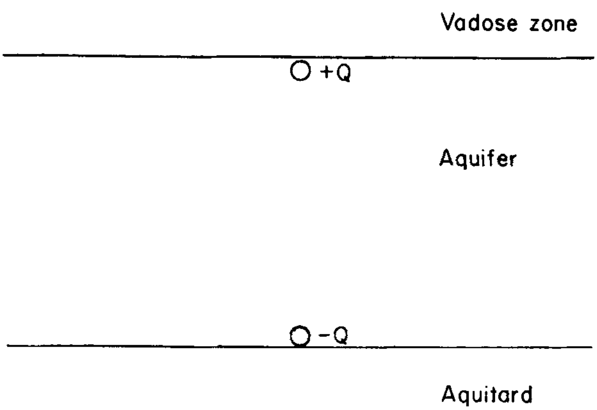

FIG. 2. Locations of source and sink representing the water intake and discharge of a sparging well.

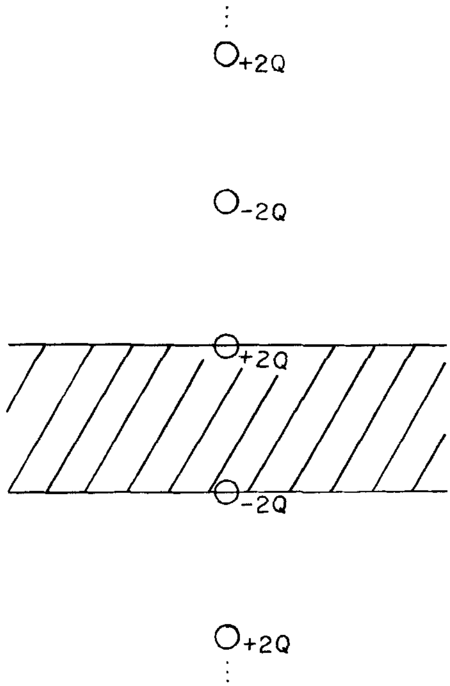

FIG. 3. Distribution of sources and sinks for generating the water flow field in the vicinity of a sparging well by the method of images. The hatched region represents the domain of physical interest.

which yields $A = 1/4\pi$. Then

$$W = \sum_{n=-\infty}^{\infty} \frac{Q}{2\pi} \left[\frac{1}{\{r^2 + [z - (2n + 1)h]^2\}^{1/2}} - \frac{1}{\{r^2 + [z - 2nh]^2\}^{1/2}} \right] \tag{29}$$

Now the linear velocity of the fluid is given by

$$v = -\frac{1}{\nu} \nabla W \tag{30}$$

This gives for the velocity components v_r and v_z the following results:

$$v_r = \frac{Q}{2\pi\nu} \sum_{n=-\infty}^{\infty} \left[\frac{r}{\{r^2 + [z - (2n + 1)h]^2\}^{3/2}} - \frac{r}{\{r^2 + [z - 2nh]^2\}^{3/2}} \right] \tag{31}$$

and

$$v_z = \left[\frac{Q}{2\pi\nu} \sum_{n=-\infty}^{\infty} \frac{z - (2n + 1)h}{\{r^2 + [z - (2n + 1)h]^2\}^{3/2}} - \frac{z - 2nh}{\{r^2 + [z - 2nh]^2\}^{3/2}} \right] \tag{32}$$

The flow paths and transit times are then calculated by integrating the parametric equations

$$dr/dt = v_r(r,z) \tag{33}$$

and

$$dz/dt = v_z(r,z) \tag{34}$$

Streamlines (flow paths) for such a system are shown in Fig. 4. The parameters used in calculating these, the transit time of each of the streamlines shown, and the volumes enclosed by the figures of revolution generated by rotating the streamlines around the axis between the sink and the source are shown in Table 3. A dimensionless time $\tau = h^3t/Q$ and a dimensionless distance $x' = x/h$ can be used to calculate from Fig. 4 and Table 3 the transit times for geometrically similar streamlines with different values of the aquifer thickness h and the flow rate Q. We see from Table

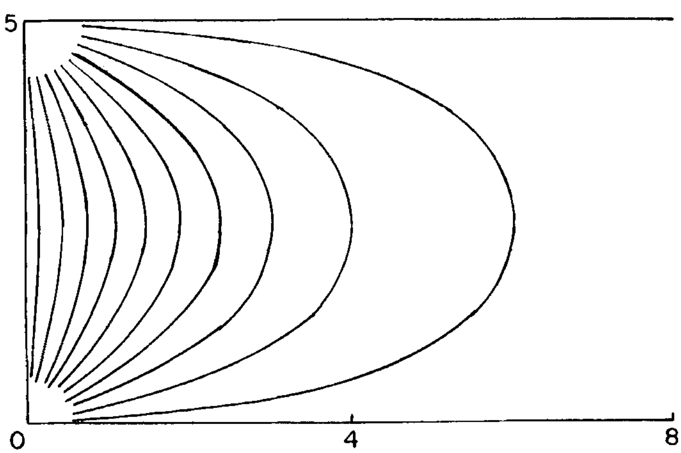

FIG. 4. Streamlines in an aquifer in the vicinity of a single sparging well. The parameters used and the transit times along each of the streamlines are given in Table 3.

TABLE 3
Streamlines and Transit Times around a Sparging Well (see Fig. 4)

Thickness of aquifer = 5 m
Aquifer porosity = .3
Induced water flow rate Q_w = .01 m^3/s
Radius of domain = 8 m

i	Transit time (s)	R_{max} of streamline (m)	Volume contained within surface generated by rotating streamline (m^3)
1	1,490	0.147	0.156
2	1,580	0.445	1.441
3	1,770	0.755	4.198
4	2,110	1.086	8.867
5	2,680	1.452	16.254
6	3,690	1.872	27.995
7	5,610	2.379	47.354
8	9,780	3.036	81.812
9	21,930	4.003	154.294
10	104,650	6.003	394.710

3 that a volume around the sparging well of approximately $1.2h^3$ is flushed out fairly rapidly (within about 6 h with these parameters), but that the flushing time increases very markedly up to 29 h if the volume of influence of the well is increased to a value of $3.2h^3$. Evidently the effective radius of influence of a sparging well is somewhere around $0.8h$.

AN *n*-COMPARTMENT SPARGING WELL MODEL

Here we use the velocity field calculated in the previous section to construct an n-compartment model for the operation of a sparging well operating in a stagnant or nearly stagnant aquifer. The set-up is shown in Fig. 5.

The flow of fluid between the ith and the $(i + 1)$th annular volume elements in the top half of the domain is given by

$$Q_i^{\text{out}} = \int_0^{2\pi} \int_{h/2}^{h} \nu v_r \cdot r_i d\theta dz \tag{35}$$

$$= Qr_i^2 \int_{h/2}^{h} \left[\sum_{n=-\infty}^{\infty} \{r_i^2 + [z - (2n + 1)h]^2\}^{-3/2} - \{r_i^2 + [z - 2nh]^2\}^{-3/2} \right] dz \tag{36}$$

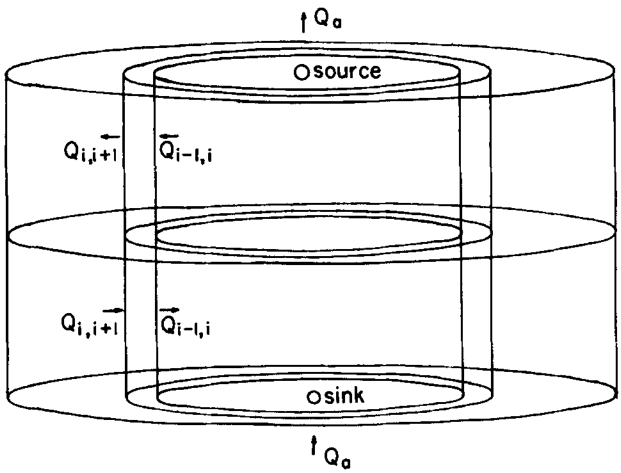

FIG. 5. An n-compartment sparging well model, showing the partitioning of the domain in the vicinity of the sparging well into $2n$ annular volume elements.

Integration and insertion of the limits of integration then yield

$$Q_i^{\text{out}} = Q \sum_{n=-\infty}^{\infty} \left[\frac{-1}{\{1 + [r_i/2nh]\}^{1/2}} + \frac{1}{\{1 + [r_i/(2n + \frac{1}{2})]^2\}^{1/2}} + \frac{1}{\{1 + [r_i/(2n - 1)h]^2\}^{1/2}} - \frac{1}{\{1 + [r_i/(2n - \frac{1}{2})h]^2\}^{1/2}} \right] \tag{37}$$

as the flow rate outward from the ith to the $(i + 1)$th annular volume element in the top half of the domain. Henceforth we denote this as $Q_{i,i+1}$. Note that here the individual series do not converge; it is necessary to pair positive and negative terms in order to get a convergent series.

We note that in the bottom half of the domain the flow rates are the same in magnitude but in the opposite direction (from the periphery toward the well). We use these flow rates to get an estimate of the movement of dissolved VOC between the volume elements by advection. This, together with the assumption that the central volume element is being sparged with air at a flow rate Q_a, that this volume element is well-mixed, and that Henry's law applies, yields the following model equations for the sparging system:

$$V_i \frac{dc_i}{dt} = Q_{i-1,i}(c_{i-1} - c_i) + Q_{i,i+1}(c_{i+1} - c_i), \qquad i = 2, 3, \ldots \tag{38}$$

and

$$V_1\frac{dc_1}{dt} = Q_{1,2}(c_2 - c_1) - Q_a K_H c_1 \tag{39}$$

Here V_j is the volume of the jth annular volume element,

$$V_j = [j^2 - (j - 1)^2]\pi(\Delta r)^2 h \tag{40}$$

Note that this model, as well as the two simpler ones presented above, are for handling the removal of a dissolved VOC. The models are not applicable if nonaqueous phase liquid (NAPL) is present, since in that case the rate-limiting step is almost certain to be the rate of dissolution of the nonaqueous phase liquid into the aqueous phase, which is not handled in these models. One would expect, however, that the flow velocities calculated above would be helpful in the development of a model for NAPL removal, since mass transfer from the NAPL phase is surely affected by the velocity of the water streaming past it.

RESULTS

The n-compartment model was implemented in TurboBASIC and run on microcomputers using MS-DOS, equipped with math coprocessors, and running at clock speeds between 12 and 33 MHz. Run times ranged from 15 minutes to about an hour, depending on the run parameters.

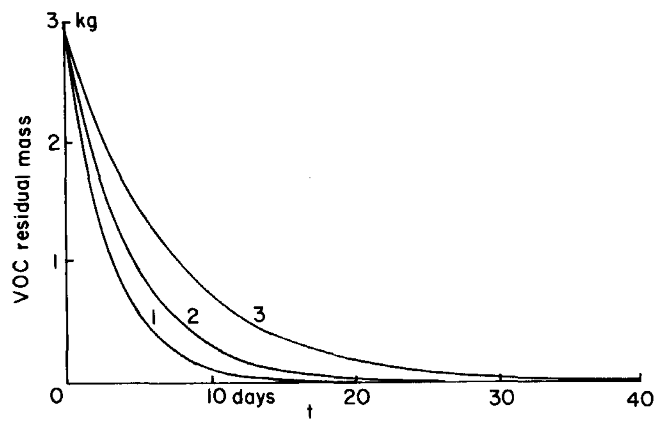

FIG. 6. VOC sparging simulation using the n-compartment model. Effect of air flow rate on removal rate of VOC. See Table 4 for default run parameters. Q_a = 0.01, 0.005, and 0.0025 m^3/s for Runs 1, 2, and 3, respectively.

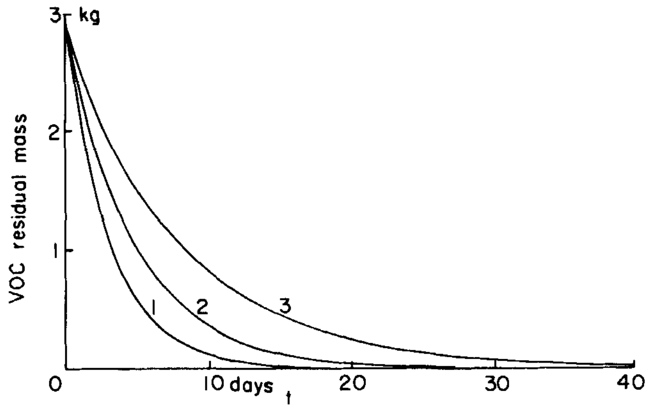

FIG. 7. VOC sparging simulation using the n-compartment model. Effect of water flow rate on removal rate of VOC. See Table 4 for default run parameters. Q_w = 0.01, 0.005, and 0.0025 m^3/s for Runs 1, 2, and 3, respectively.

Default parameters for all of the runs shown in Figs. 6–8 are given in Table 4. Values of parameters having values other than the default values are given in the captions. Figure 6 illustrates the effect of varying the water flow rate Q_w, and shows the expected increase in VOC removal rate with increasing Q_w. In these runs the air flow rate Q_a was held constant.

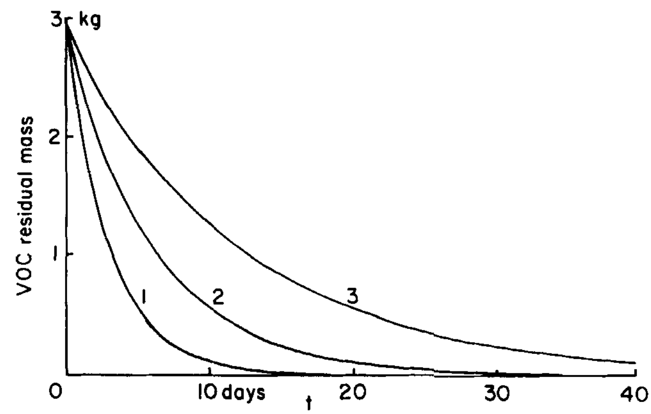

FIG. 8. VOC sparging simulation using the n-compartment model. Effect of linked water and air flow rates on removal rate of VOC. See Table 4 for default run parameters. In these runs Q_a = Q_w = 0.01 (Run 1), 0.005 (Run 2), and 0.0025 m^3/s (Run 3).

TABLE 4
Default Parameters for the Runs Plotted in Figs. 6–9[a]

Domain radius = 5 m
Aquifer thickness = 5 m
Radius of zone of contamination = 5 m
Number of annular compartments = 20
Air flow rate Q_a = .01 m^3/s
Water circulation rate Q_w = .01 m^3/s
Henry's constant = .1 (dimensionless)
Porosity of aquifer medium = .3
Initial VOC concentration in groundwater = 25 mg/L

[a]Departures from these values are indicated in the captions of the figures.

The effect of varying the air flow rate Q_a is shown in Fig. 7. Here Q_w was held constant. The expected increase of removal rate with increasing air flow rate is observed. Air and water flow rates Q_a and Q_w are varied together in the runs shown in Fig. 8; Q_a was taken equal to Q_w in these three runs. The VOC removal rate appears to be proportional to Q_a for these runs. In fact one would expect Q_w to be linked to Q_a in some fashion such as this.

The effect of varying the Henry's constant of the VOC is shown in Fig. 9. Removal rate increases with increasing Henry's constant, but is not proportional to K_H with the parameter sets used here.

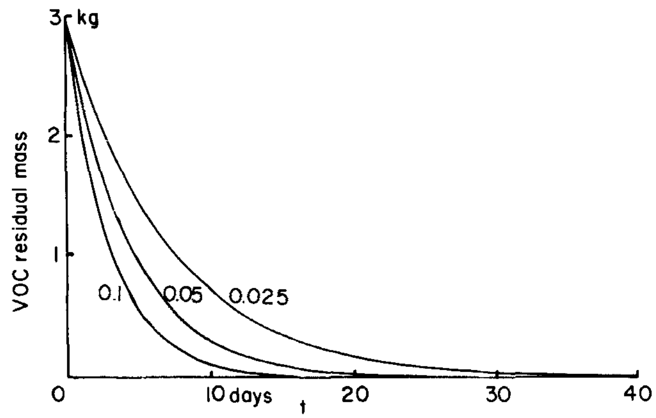

FIG. 9. VOC sparging simulation using the n-compartment model. Effect of Henry's constant. Default run parameters are given in Table 4. Henry's constants are 0.1, 0.05, and 0.025 as indicated.

We note that the manner in which Q_w depends on Q_a is likely to be highly site specific, depending particularly on the permeability of the aquifer. One can reasonably expect that Q_w increases monotonically with increasing Q_a, but the precise functional form of this dependence is expected to be site specific. Use of this model is therefore dependent upon the availability of pilot test data giving information on the dependence of the induced water flow rate Q_w on the air sparging rate Q_a.

REFERENCES

1. B. Herrling and J. Stamm, *Vacuum-Vaporizer-Wells (UVB) for In Situ Remediation of Volatile and Strippable Contaminants in the Unsaturated and Saturated Zones*, Presented at the Symposium on Soil Venting, Houston, Texas, April 29–May 1, 1991, Robert S. Kerr Environmental Research Laboratory and National Center for Ground Water Research, sponsors.
2. R. A. Brown, *Air Sparging—Extending Volatilization to Contaminated Aquifers*, Presented at the Symposium on Soil Venting, Houston, Texas, April 29–May 1, 1991, Robert S. Kerr Environmental Research Laboratory and National Center for Ground Water Research, sponsors.
3. D. J. Wilson, S. Kayano, R. D. Mutch Jr., and A. N. Clarke, "Groundwater Cleanup by *in-situ* Sparging. I. Mathematical Modeling," *Sep. Sci. Technol.*, *27*, 1023 (1992).
4. S. E. Powers, C. O. Louriero, L. M. Abriola, and W. J. Weber Jr., "Theoretical Study of the Significance of Nonequilibrium Dissolution of Nonaqueous Phase Liquids in Subsurface Systems," *Water Resour. Res.*, *27*, 463 (1991).

Received by editor March 25, 1992